Departement für Pferde, Klinik für Pferdechirurgie
der Vetsuisse-Fakultät Universität Zürich

Direktor: Prof. Dr. med. vet. Anton Fürst, Dipl. ECVS

Arbeit unter der wissenschaftlichen Betreuung von
Dr. med. vet. Michelle Jackson, Dipl. ECVS

Comparison of radiography and computed tomography for the detection of subchondral cystic lesions in the limbs of horses

Inaugural-Dissertation

zur Erlangung der Doktorwürde der
Vetsuisse-Fakultät Universität Zürich

vorgelegt von

Stephanie Schön

Tierärztin
von Menzingen, Zug

genehmigt auf Antrag von

Prof. Dr. med. vet. Anton Fürst, Dipl. ECVS, Referent
Prof. Dr. med. vet. Patrick Robert Kircher, Dipl. ECVDI, Korreferent

2015

Meinen Eltern Hugo und Ruth Schön,
sowie meinem lieben Freund Raffael Weber,
welche mich immer grosszügig unterstützen

Content

1 Summary

The objective of this study was to describe radiographic and computed tomographic characteristics of subchondral cystic lesions (SCLs) that were identified on computed tomography (CT) scans and to compare the two imaging techniques with respect to the diagnosis of SCLs.

Horses presented because of an SCL and with a complete radiographic and CT examination of the affected joint were included. Radiographs and CT images were evaluated with respect to the following criteria: localization and size of the SCL, communication between the SCL and the joint, fissures, presence of small channels, additional osteoarthritic changes (OA) and periosteal reaction (PR).

Thirty-four horses with 45 SCLs were included in the study. Radiography allowed detection of 78% of the SCLs (n=35) and concomitant fissures in 16% of the cases (n=7). Computed tomography showed a connection with the overlying cartilage in over 96% of all SCLs (n=43) and a concomitant fissure in 29% (n=13) of the cases. One third of the SCLs were associated with a wide channel, which was only visible with CT.

This study highlights the advantages of CT over digital radiography for the detection of SCLs in horses. Most of the SCLs communicated with the joint and about one third were associated with a fissure. Channel formation seen with CT seems to be a frequent additional feature of SCLs.

2 Zusammenfassung

Das Ziel dieser Studie bestand darin, subchondrale Knochenzysten (SK) der Gliedmasse des Pferdes mittels Röntgen und Computertomographie (CT) zu beurteilen und gegenseitig zu vergleichen.

Alle Pferde mit einer SK und einer vollständigen radiologischen und computertomographischen Untersuchung wurden eingeschlossen. Die Röntgen- und CT-Bilder wurden nach folgenden Kriterien beurteilt: Lokalisation und Grösse der Zysten, Verbindung der SK mit dem Gelenk, Fissurbildung, das Vorkommen von feinen Kanälen im Zusammenhang mit den SK sowie zusätzliche arthrotische Veränderungen.

Es wurden insgesamt 34 Pferde mit 45 SK untersucht, wobei radiologisch nur 78% (n=35) der SK diagnostiziert werden konnten. Eine zusätzliche Fissur konnte radiologisch bei 16% (n=7) und im CT bei 29% (n=13) der SK gefunden werden. Zudem hat die CT Untersuchung in 96% der SK eine Gelenksverbindung gezeigt (n=43) und bei einem Drittel aller SK (33%) wurden erweiterte Kanäle gefunden.

Mit dieser Arbeit wurden die Vorteile des CTs gegenüber der digitalen Radiographie für die Diagnose und Beurteilung von SK gezeigt. Die meisten Zysten stehen über eine Öffnung mit dem Gelenksknorpel in Verbindung und oft konnte eine zusätzliche Fissur dargestellt werden. Die mittels CT definierten Kanäle, ausgehend von den SK, müssen histologisch weiter untersucht werden.

3 Thesis Monography

3.1 Introduction

Subchondral cystic lesions (SCLs) are common in horses and often cause lameness.[1,2] They are most frequently found in the medial femoral condyle (45.8%), phalanges (26.2%), and carpus (7.1%).[3] Radiographs are often diagnostic and show the size and shape of the cyst and possible communication between the cysts and the joint cavity. A typical radiographic finding is a dome-shaped or round to oval subchondral lucency with a variable sclerotic rim. Additional findings such as fissures, osteoarthritis of the affected joint, or periarticular new bone formation are important in terms of therapy and prognosis. Unfortunately, radiographs are not always diagnostic in horses with SCLs because of summation of opacities and complex anatomical features. A change in bone density of at least 30 to 50% is required for the radiographic identification of osseous lesions[2,4] and therefore small SCLs and fissures may be missed. Furthermore, the accurate assessment of the communication between the SCL and the overlying cartilage can be difficult.[5] Determination of the exact localization of the SCLs is critical for the surgical approach and radiographs are not always accurate for this purpose.[4] For these reasons, other diagnostic imaging modalities are indispensable when SCLs are suspected.

Ultrasonographic evaluation can provide additional information about the relationship between SCLs and the joint, for instance the fetlock or stifle joint.[6] Jacquet et al. reported that all SCLs of the medial femoral condyle diagnosed radiographically were visible ultrasonographically, whereas some small lesions identified ultrasonographically were not clearly visible on radiographs.[6] Bone scintigraphy is a very sensitive tool for detection of early bone changes including SCLs.[7,2] Magnetic resonance tomography (MRT) also has been used to diagnose SCLs in the distal limbs of horses[7,8] but subtle cartilaginous changes and fissure lines cannot always be visualized using this technique.[9]

Computed tomography (CT) is a superior diagnostic imaging tool that allows accurate evaluation of osseous structures, without superimposition of other structures, in the distal limbs of horses.[10,11] Subchondral cystic lesions can be

precisely located[4] and other lesions such as fissures and arthritic changes or the communication between the cyst and joint space can be assessed. Osseous lesions that may be missed or only partially assessed radiographically can be fully characterized using CT.[2,4,12,13]

The purpose of this study was to compare the accuracy of radiography and CT for the diagnosis of SCLs in the limbs of horses. We hypothesized that CT is superior to radiography for the detection of SCLs, the assessment of the communication between the cysts and the adjacent joint space, and the detection of fissures involving the joint, which are easily missed radiographically.

3.2 Materials and Methods

This retrospective study evaluated the medical records of horses admitted to the Vetsuisse Faculty of Zurich, Switzerland, because of an SCL of the phalanges, third metacarpal and metatarsal bones (MC/MT III), and radial carpal bone (RCB) diagnosed using CT between 2005 and 2014. Subchondral cystic lesions of the distal and proximal sesamoid bones were not considered. All horses had undergone routine orthopedic examination and complete radiographic (FCR Profect CS, Fujifilm, Zurich, Switzerland) and computed tomographic examination of the affected region of the limb. A 40-slice helical CT scanner (Somatom Sensation Open, Siemens Medical Solutions, Zurich, Switzerland) was used for the latter with the horses under general anesthesia. The images were evaluated with a dedicated DICOM viewer (OsiriX 64-bit, OsiriX Foundation, Geneva, Switzerland).

3.2.1 Radiography

One lateromedial, one dorsopalmar/dorsoplantar, and two oblique radiographic views of each affected joint were taken and the following parameters determined: exact location of the SCL within the bone (proximal, distal, medial, lateral or sagittal), shape of the SCL (round, oval, half-circle, pear-shaped, conical or shapeless), content (homogeneous or heterogeneous), surrounding sclerosis (no, slight, moderate or severe sclerosis), presence of a fissure, and communication between the cyst and joint space. An SCL with a wide or small neck-like opening to the joint was considered to communicate with the joint space, whereas a SCL located at a certain distance from the joint surface and with no obvious connection was considered not to communicate. Other radiographic features including periarticular reactions (PR) and osteoarthrosis (OA) in the adjacent joint (both graded as no, mild, moderate or severe changes) were evaluated independent of the radiographic assessment of SCLs.

The cross-sectional area of the cystic lesion (cm^2) was calculated using the measurement tools included in Osirix. Because of the retrospective nature of

the study, markers for calculation of the true SCL area were not used. Radiographs were evaluated before the CT images.

3.2.2 Computed tomography

The assessment of SCLs on CT scans was analogous to the assessment on radiographs. The SCLs were evaluated in three planes (transverse, sagittal and dorsal) but evaluation of the shape and measurements of the cross-sectional area of the cysts were carried out in the dorsal plane as on the radiographs. Scans were also assessed for the presence of channels between the SCL and the cortex. These channels did not involve the joint.

3.2.3 Statistical Analysis

The SPSS statistical program (IBM SPSS Statistics, Version 19, Chicago, Illinois, USA) was used for descriptive statistical analysis. Univariate analysis compared the SCLs with the previously mentioned variables using Fisher's exact test after creation of contingency tables. Differences were considered significant at $P \leq 0.05$. Logistic regression was used for further evaluation of correlation of the mentioned variables with the SCLs. Cystic lesions were divided into four groups: solitary SCL, two SCLs in different legs, two SCLs in the same joint, and two SCLs in different joints in the same leg. Univariate analyses and logistic regression were carried out using Stata Software (StataCorp, 2011; Stata Statistical Software: Release 12; College Station, TX, USA: StataCorp LP).

3.3 Results

Thirty-four horses with a total of 45 SCLs fulfilled the inclusion criteria for the study (Table 1a and b). The horses had a mean age of 8.2±4.0 years (range, 1 to 16 years), and there were 14 mares, 18 geldings, and 2 stallions. Breeds included 26 (76%) Warmblood horses, 3 (9%) Quarter Horses, 2 (6%) ponies, 1 (3%) Haflinger, 1 Friesian, and 1 Icelandic horse.

Computed tomography showed 45 SCLs in a total of 41 joints (4 joints had 2 SCLs): Forelimbs (13 joints in the left forelimb and 14 joints in the right forelimb) were more often affected than hind limbs (8 joints in the left hind limb and 6 joints in the right hind limb). Of the 34 horses, 23 had a single SCL and 11 had more than one SCL: 5 horses had a second SCL in a different leg, 4 horses had a second SCL in the same joint but in a different bone, and 2 horses had a second SCL in the same leg but in a different joint.

Table 1a) Overview of evaluation criteria of the SCLs. Prox = proximal, Dist = distal, RCB = radiocarpal bone, MC III = third metacarpal bone, MT III = third metatarsal bone, Sag = sagittal, Med = medial, Lat = lateral, Cent = centrally, SL=shapeless, HC = half-circle, PS = pear-shaped, H = homogeneous, IH = heterogeneous

Nr	Visibility		Localization				Size (cm^2)		Shape		Content	
	Rx	CT	Rx	CT	Rx	CT	Rx	CT	Rx	CT	Rx	CT
1	Yes	Yes	Dist P1	Dist P1	Lat	Lat	0.17	0.19	Oval	Oval	H	H
2	No	Yes	-	Prox P1	-	Sag	-	0.08	-	SL	-	IH
	No	Yes	-	Dist MCIII	-	Sag	-	0.12	-	SL	-	IH
3	Yes	Yes	Dist P1	Dist P1	Med	Med	0.42	0.41	HC	Round	IH	IH
4	Yes	Yes	Prox P3	Prox P3	Sag	Sag	1.66	1.72	Round	Round	H	H
	Yes	Yes	Prox P3	Prox P3	Sag	Sag	0.50	0.83	SL	PL	IH	IH
5	Yes	Yes	Dist MCIII	Dist MCIII	Med	Med	0.53	0.37	SL	SL	IH	IH
6	Yes	Yes	Prox P1	Prox P1	Sag	Sag	0.16	0.14	SL	SL	IH	IH
7	Yes	Yes	RCB	RCB	Cent	Cent	1.60	1.62	Oval	Oval	H	H
	Yes	Yes	Prox P1	Prox P1	Sag	Sag	0.29	0.23	Round	Round	H	H
8	Yes	Yes	Prox P1	Prox P1	Sag	Sag	0.16	0.26	Round	SL	IH	IH
	Yes	Yes	Prox P1	Prox P1	Sag	Sag	0.28	0.20	SL	SL	IH	IH
9	Yes	Yes	Dist P1	Dist P1	Sag	Sag	0.46	0.20	SL	SL	IH	IH
10	No	Yes	-	Prox P1	-	Lat	-	0.14	-	SL	-	IH
	No	Yes	-	Prox P1	-	Sag	-	0.15	-	SL	-	IH
11	Yes	Yes	Dist MTIII	Dist MTIII	Med	Med	0.40	0.28	SL	SL	H	IH
	No	Yes	-	Prox P1	-	Med	-	0.33	-	HC	-	IH
12	Yes	Yes	Prox P1	Prox P1	Sag	Sag	0.16	0.17	Round	Round	IH	IH
	Yes	Yes	Prox P1	Prox P1	Sag	Sag	0.62	0.19	Round	Round	H	IH
13	Yes	Yes	Dist MCIII	Dist MCIII	Lat	Lat	0.12	0.16	SL	SL	H	IH
14	Yes	Yes	Prox P2	Prox P2	Lat	Lat	0.37	0.31	Conical	Round	H	IH
15	Yes	Yes	Prox P3	Prox P3	Sag	Sag	1.04	0.81	SL	SL	IH	IH
16	Yes	Yes	Prox P1	Prox P1	Med	Med	0.24	1.15	Oval	Oval	IH	IH
17	Yes	Yes	Prox P1	Prox P1	Sag	Sag	0.06	0.07	SL	SL	IH	IH
18	No	Yes	-	Dist MCTIII	-	Med	-	0.24	-	SL	-	IH
19	Yes	Yes	Prox P1	Prox P1	Med	Med	0.28	0.09	SL	Oval	IH	IH
20	Yes	Yes	Prox P3	Prox P3	Sag	Sag	0.23	0.58	SL	SL	IH	IH
	No	Yes	Prox P3	Prox P3	Sag	Sag	-	0.32	-	SL	-	IH
21	Yes	Yes	Dist P1	Dist P1	Sag	Sag	1.36	0.84	SL	SL	IH	IH
22	Yes	Yes	Prox P3	Prox P3	Med	Med	0.29	0.54	Oval	Round	H	IH
23	Yes	Yes	Prox P1	Prox P1	Med	Med	0.14	0.34	SL	SL	IH	IH
24	Yes	Yes	RCB	RCB	Cent	Cent	0.94	0.91	Round	Oval	H	H
25	Yes	Yes	Prox P1	Prox P1	Sag	Sag	0.20	0.32	Round	SL	H	H
26	Yes	Yes	Dist MCIII	Dist MCIII	Sag	Sag	0.06	0.36	Round	SL	H	IH
	No	Yes	-	Prox P1	-	Sag	-	0.23	-	SL	-	IH
27	Yes	Yes	Dist P2	Dist P2	Lat	Lat	1.77	0.90	Round	Round	IH	IH
	No	Yes	-	Prox P2	-	Sag	-	0.18	-	PL	-	IH
28	Yes	Yes	Prox P3	Prox P3	Sag	Sag	0.51	0.36	Round	Round	H	H
29	Yes	Yes	Prox P1	Prox P1	Sag	Sag	0.14	0.16	HC	SL	H	IH
30	Yes	Yes	Prox P1	Prox P1	Sag	Sag	0.19	0.12	SL	SL	IH	H
31	Yes	Yes	Prox P1	Prox P1	Med	Med	0.27	0.41	SL	SL	IH	IH
32	Yes	Yes	Prox P1	Prox P1	Sag	Sag	0.16	0.13	HC	SL	IH	IH
33	No	Yes	-	Dist MTIII	-	Sag	-	0.25	-	Round	-	IH
34	Yes	Yes	Dist P1	Dist P1	Sag	Sag	1.17	0.99	Oval	Round	H	H
	Yes	Yes	Dist P1	Dist P1	Sag	Sag	0.56	0.52	Round	Round	H	H

Table 1b) Overview of all evaluation criteria of the SCLs. OA = osteoarthrosis, PR = periosteal reactions, Md = mild, Mt = moderate, S = severe, C = channel

Nr	Visibility		Surrounding sclerosis		Synovial connection		Fissure Channel		OA		PR	
	Rx	CT	Rx	CT	Rx	CT	Rx	CT	Rx	CT	Rx	CT
1	Yes	Yes	Md	Mt	Yes	Yes	Yes	C	No	No	No	No
2	No	Yes	-	Md	-	Yes	No	Yes	Md	Md	No	MT
	No	Yes	-	Md	-	Yes	No	No	Md	Md	No	MT
3	Yes	Yes	Md	Md	Yes	Yes	Yes	C	No	Md	Md	Md
4	Yes	Yes	Mt	Md	Yes	Yes	No	No	No	No	No	No
	Yes	Yes	No	Md	Yes	Yes	No	No	No	No	No	No
5	Yes	Yes	No	Mt	Yes	Yes	No	C	Mt	Mt	No	No
6	Yes	Yes	Mt	Mt	Yes	Yes	Yes	Yes	Md	Md	Md	Md
7	Yes	Yes	Md	Md	No	Yes	No	C	No	No	No	Md
	Yes	Yes	Md	Mt	Yes	Yes	No	No	Mt	No	No	No
8	Yes	Yes	Mt	Mt	Yes	Yes	No	Yes	Md	Md	No	No
	Yes	Yes	Mt	Mt	Yes	Yes	No	Yes	Md	Md	No	No
9	Yes	Yes	No	No	Yes	Yes	No	Yes	No	No	No	Md
10	No	Yes	-	Md	-	Yes	No	No	No	Md	No	No
	No	Yes	-	Md	-	Yes	No	No	No	Md	No	No
11	Yes	Yes	Md	Mt	No	Yes	No	No	Md	Md	No	No
	No	Yes	-	No	-	Yes	No	No	Md	Md	No	No
12	Yes	Yes	S	S	Yes	Yes	No	Yes	Mt	Mt	No	No
	Yes	Yes	Mt	Md	Yes	Yes	No	No	Mt	Md	No	No
13	Yes	Yes	No	Mt	No	Yes	No	C	Md	Md	No	No
14	Yes	Yes	No	No	Yes	Yes	No	C	Md	No	No	No
15	Yes	Yes	No	No	Yes	Yes	Yes	Yes	No	Md	No	No
16	Yes	Yes	Mt	Mt	Yes	Yes	No	C	Mt	Mt	S	S
17	Yes	Yes	Mt	Md	Yes	Yes	Yes	Yes	Md	Md	No	Md
18	No	Yes	-	Md	-	Yes	No	No	No	No	Mt	Md
19	Yes	Yes	Mt	Md	No	Yes	No	C	Md	Md	No	No
20	Yes	Yes	No	Md	Yes	Yes	No	C	No	No	No	No
	No	Yes	-	Md	-	Yes	-	C	No	No	No	No
21	Yes	Yes	Md	Mt	No	No	No	No	No	Md	No	No
22	Yes	Yes	No	No	Yes	Yes	No	No	No	No	No	No
23	Yes	Yes	Md	Md	No	Yes	No	C	No	Md	Mt	S
24	Yes	Yes	Md	Md	Yes	Yes	No	C	No	No	No	No
25	Yes	Yes	Md	Md	Yes	Yes	Yes	Yes	No	Md	Mt	S
26	Yes	Yes	No	Md	No	No	No	No	Md	Md	No	No
	No	Yes	-	Md	-	Yes	No	Yes	Md	Md	No	Md
27	Yes	Yes	Md	Mt	Yes	Yes	No	C	No	No	No	No
	No	Yes	-	Md	-	Yes	No	C	No	No	No	No
28	Yes	Yes	Md	Md	Yes	Yes	No	No	No	No	No	No
29	Yes	Yes	Mt	Mt	Yes	Yes	No	Yes	No	No	No	Md
30	Yes	Yes	Md	Md	Yes	Yes	No	Yes	Md	Mt	No	Md
31	Yes	Yes	Md	Md	No	Yes	No	C	Mt	Mt	No	No
32	Yes	Yes	Md	Md	Yes	Yes	Yes	Yes	Mt	Mt	S	S
33	No	Yes	-	Md	-	No	No	No	No	No	No	No
34	Yes	Yes	Md	Mt	Yes	Yes	No	C	No	No	No	No
	Yes	Yes	Md	Md	Yes	Yes	No	C	No	No	No	No

Cystic lesions were most often seen in the proximal first phalanx (P1, 20/45) followed by the proximal third phalanx (P3, 7/45) and the distal MC/MTIII (7/45, Fig 1). The distal P1 (6/45), proximal second phalanx (P2, 2/45), radial carpal bone (2/45), and the distal P2 (1/45) were affected less frequently. Two thirds (30 of 45, 67%) of the SCLs were in the sagittal plane, 10 (22%) were medially, and 5 (11%) were laterally (Fig 2a-c).The mean (±sd) cross-sectional area of the SCLs measured on radiographs was 0.5 ± 0.48 cm^2 (n=35) and that measured on CT images was 0.4 ± 0.39 cm^2 (n=45).

A prominent channel between the cyst and the cortex was seen on CT images of 15 (33%) SCLs (Fig 3a-c).

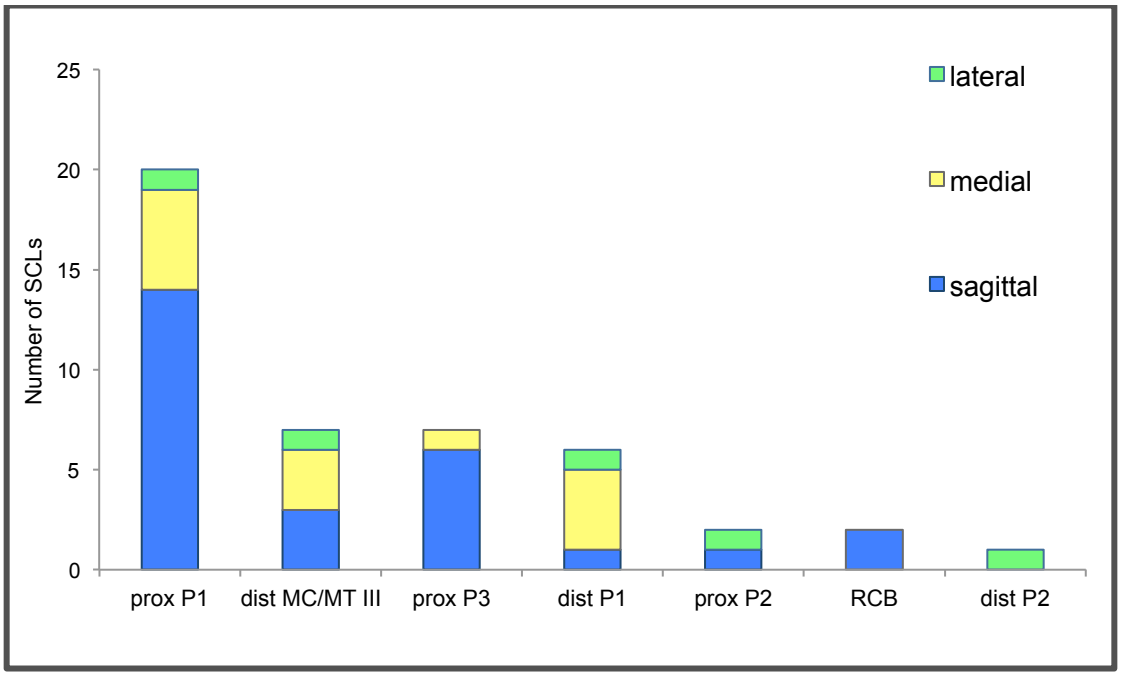

Fig 1: Distribution of SCLs within the different bones.
Prox P1 = proximal first phalanx, Dist MC/MT III = distal third metacarpal/ metatarsal bone, Prox P3 = proximal third phalanx, Prox P2 = proximal second phalanx, RCB = radial carpal bone, Dist P2 = distal second phalanx

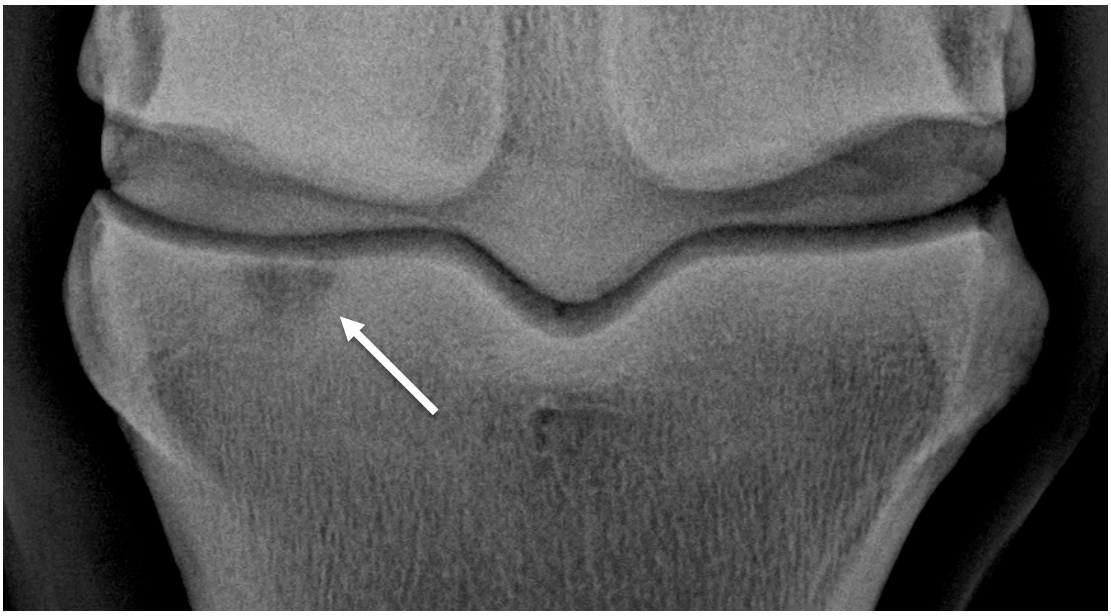

Fig 2a) Dorsopalmar radiographic view of the left fetlock of a 15-year-old Warmblood horse with acute severe lameness in the left forelimb. There is an SCL (arrow) in the medial proximal aspect of P1 with mild sclerosis and no obvious communication with the joint space.

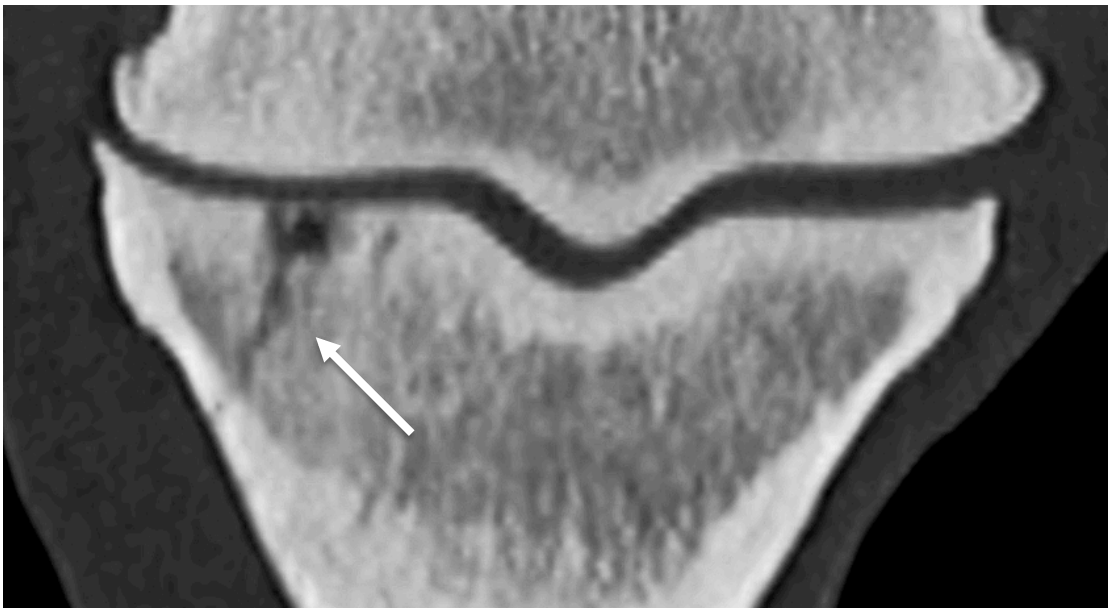

Fig 2b) Dorsal CT view of the same SCL showing a channel (arrow) between the cyst and the medial cortex of P1. Scrolling through the CT images revealed multiple channels. The cyst has an irregular margin and a heterogeneous content and communicates with the joint space. There is no fissure.

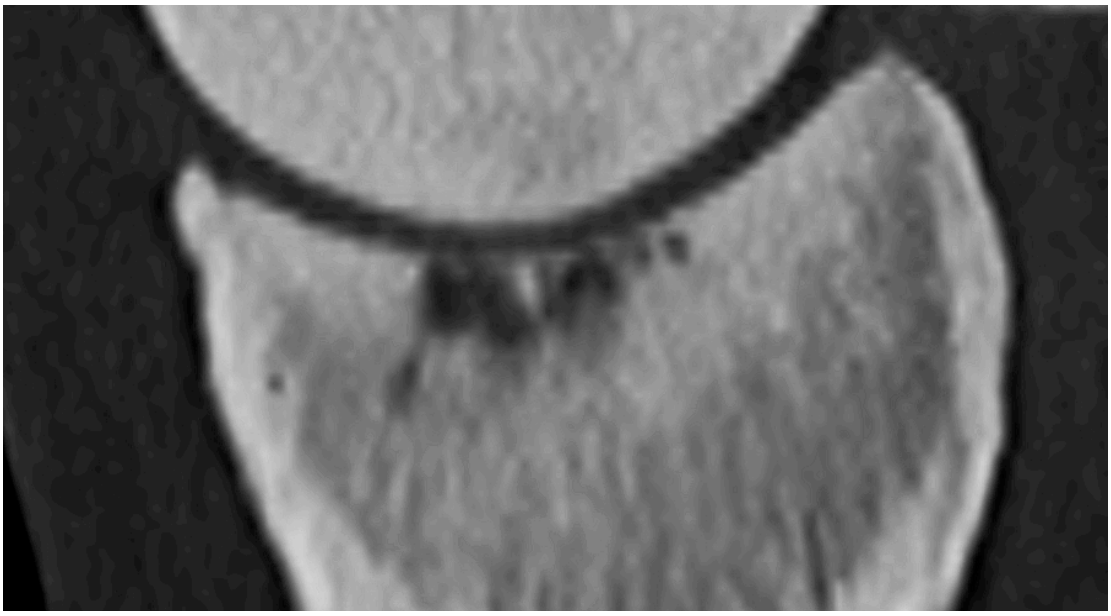

Fig 2c) Sagittal CT view of the same SCL showing heterogeneous content and mild sclerosis.

Fig 3a) Dorsopalmar radiographic view of a sagittal SCL with an obvious neck-like opening to the joint and a moderate sclerotic rim in the distal aspect of P1 of the left forelimb in a two-year-old gelding with mild intermittent lameness. The horse also had SCLs in the distal aspect of P1 of the right forelimb and an additional SCL in the right medial femoral condyle.

Fig 3b) Dorsal CT view showing the same SCL with a clear connection to the near cartilage and a kissing split-like lesion (arrow) in the opposite subchondral bone of the proximal aspect of P2. There is a marked hyperintense rim around the oval SCL.

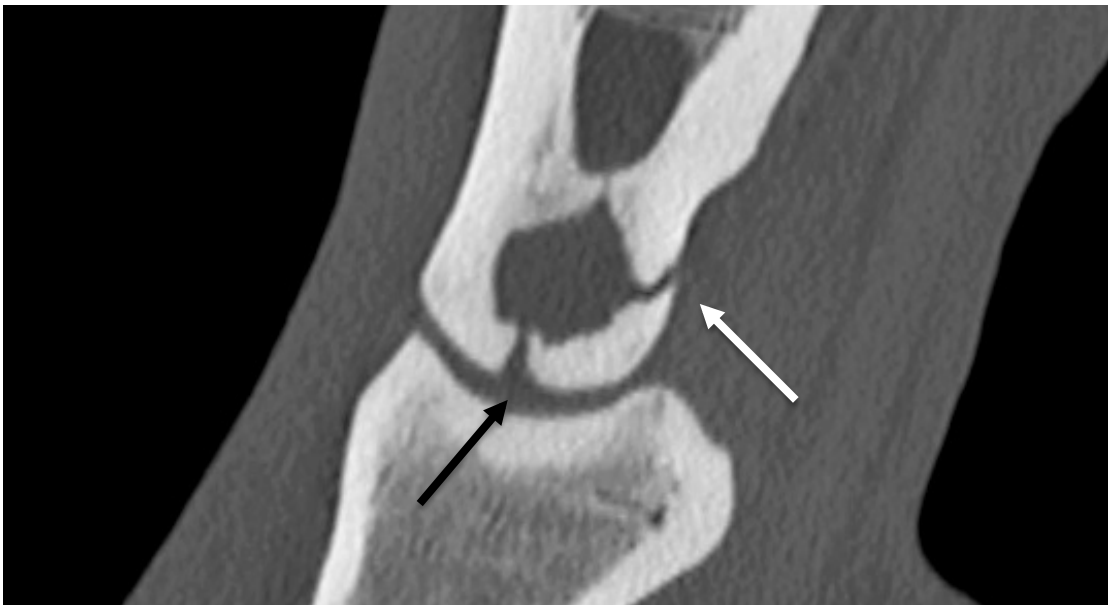

Fig 3c) The same SCLs in the sagittal plane in the CT study: A neck-like opening to the joint space (black arrow) with a wide channel exiting toward the palmar cortex (white arrow) are seen.

3.3.1 Comparison between radiography and CT

Of the 45 SCLS diagnosed by CT, 35 (78%) were identified radiographically as SCLs, whereas no obvious SCLs were detected on radiographs in the remaining 10 cases (Table 2). Computed tomography of those 10 SCLs showed no or very subtle surrounding sclerosis (univariate analysis, p=0.038 and logistic regression, OR=5.66, p=0.035). Significantly more SCLs were missed radiographically in joints with two cystic lesions (univariate analysis p=0.002 and logistic regression, OR=0.30, p=0.002).

A communication between the cyst and the joint was evident on CT scans of 43 (96%) of the 45 SCLs and was suspected in 26 (74%) of 35 SCLs seen radiographically (p=0.275, Fig 4a-c). No communication was seen on CT scans of 2 (4%) SCLs.

A fissure accompanying the SCL was detected on CT scans in 13 (29%) cases (Fig 5a-c) and was suspected on radiographs in 7 (16%) cases. Two of the latter were determined to be prominent channels when imaged by CT. Therefore, of the 13 fissure lines detected by CT, 5 were correctly diagnosed radiographically. The difference between the two imaging techniques with respect to the diagnosis of fissures was significant (p=0.015). The majority of fissure lines had a sagittal orientation (p=0.008); 11 cases occurred in the proximal aspect of P1 (p=0.045), one in the distal aspect of P1, and in one in the proximal aspect of P3.

Table 2: Comparison of radiography and CT for the diagnosis of SCLs and associated fissures, channels, and articular communications.

Variable	Evaluation criteria	X-ray (n)	CT (n)
SCL	Suspected	35	45
	Not suspected	10	0
Joint communication	Suspected	26	43
	Not suspected	9	2
	No SCL	10	0
Fissure	Suspected	7	13
	Not suspected	38	32
Channels	Suspected	0	15
	Not suspected	45	30

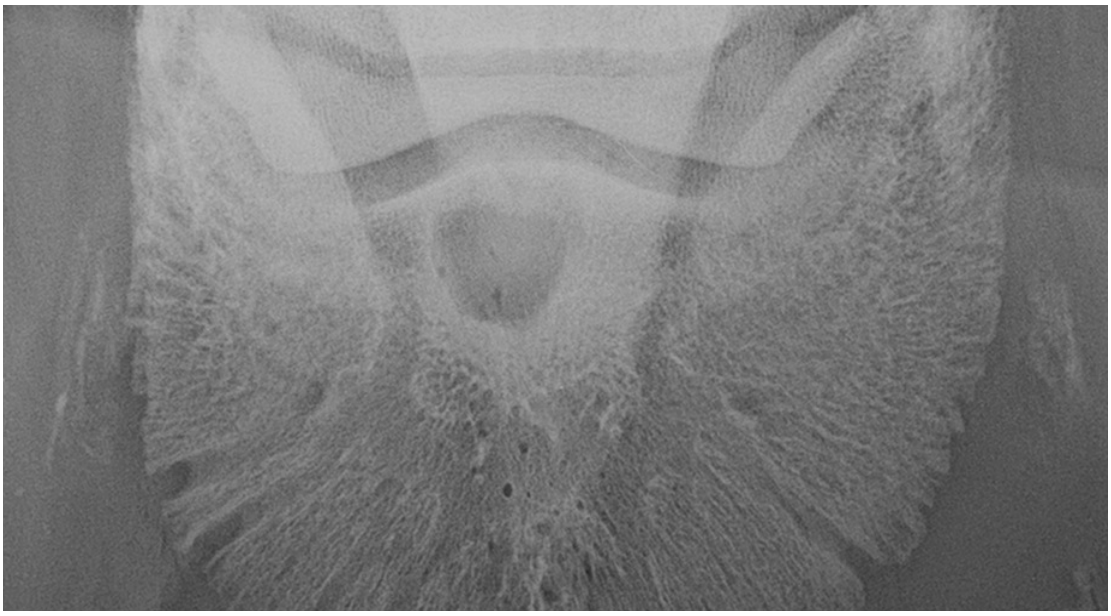

Fig 4a) Dorsal 60° proximal - palmarodistal oblique radiographic view showing an SCL in the right front P3 in an eight-year-old gelding with chronic intermittent lameness. The SCL is located proximally and sagittally and has a suspected neck-like communication with the distal interphalangeal joint.

Fig 4b) Dorsal CT view of the same SCL showing a small connection to the joint surface (arrow), a mild hyperintense rim and a homogeneous content.

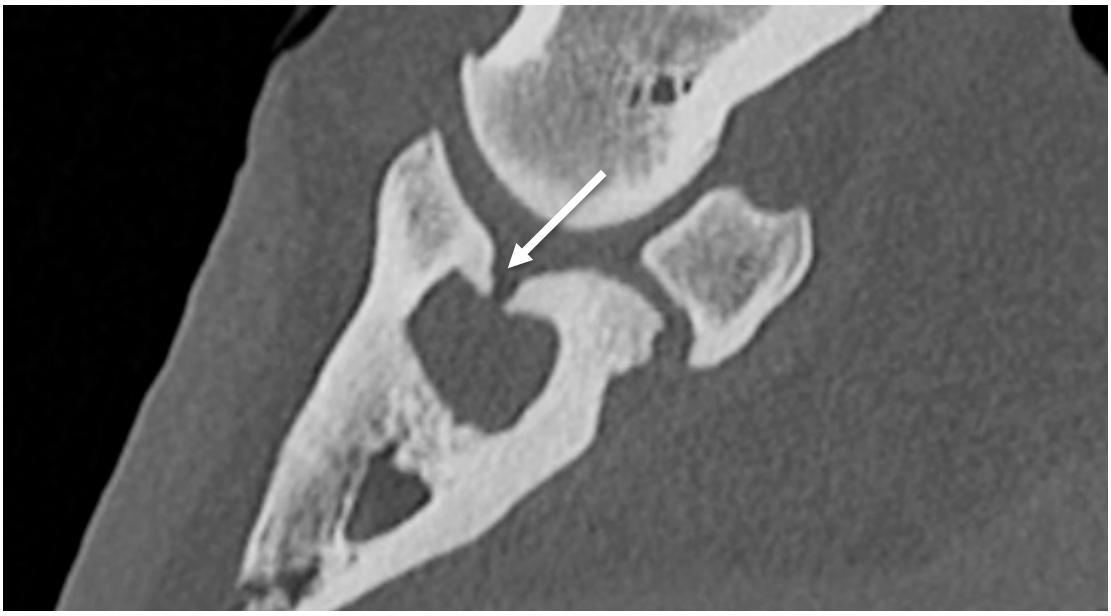

Fig 4c) CT view of the same SCL in the sagittal plane, confirming the round shape and the neck-like communication with the joint (arrow).

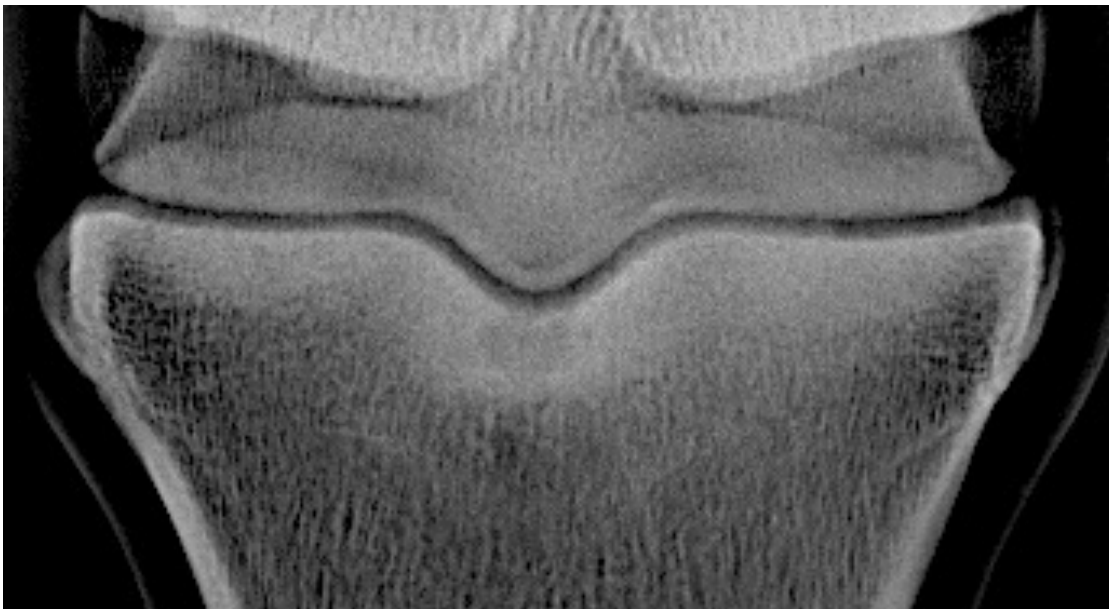

Fig 5a) Dorsopalmar radiographic view of an SCL in the proximal aspect of P1. The SCL is located sagittally and surrounded by mild sclerosis and has a suspected connection with the joint. There is no obvious radiographic fissure formation.

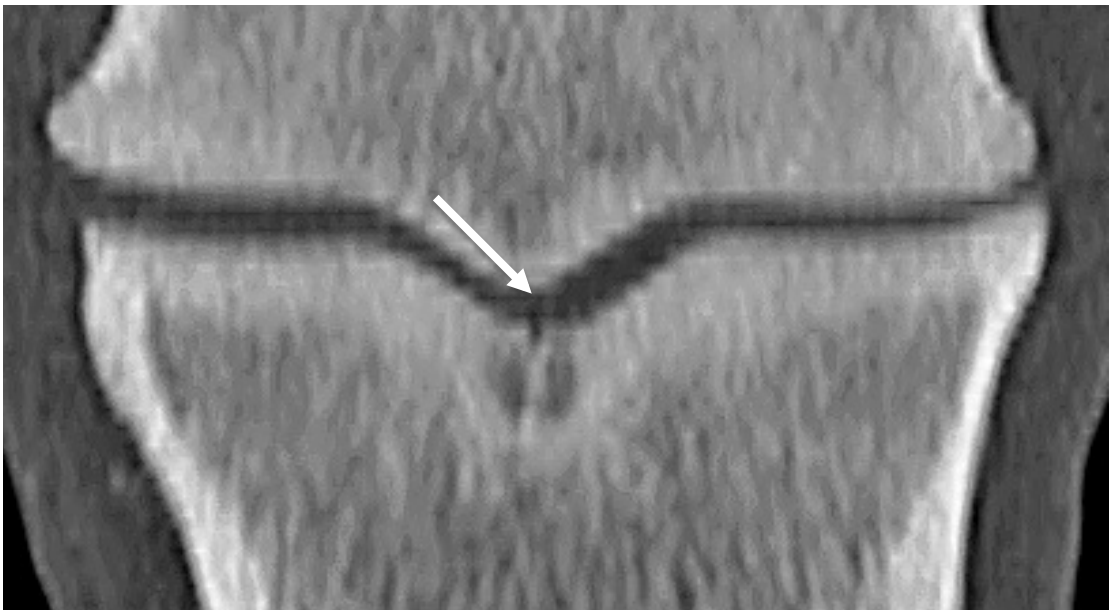

Fig 5b) Dorsal CT view of the same lesion within the proximal sagittal aspect of P1. There is a split-like crack (arrow) within the sagittal groove.

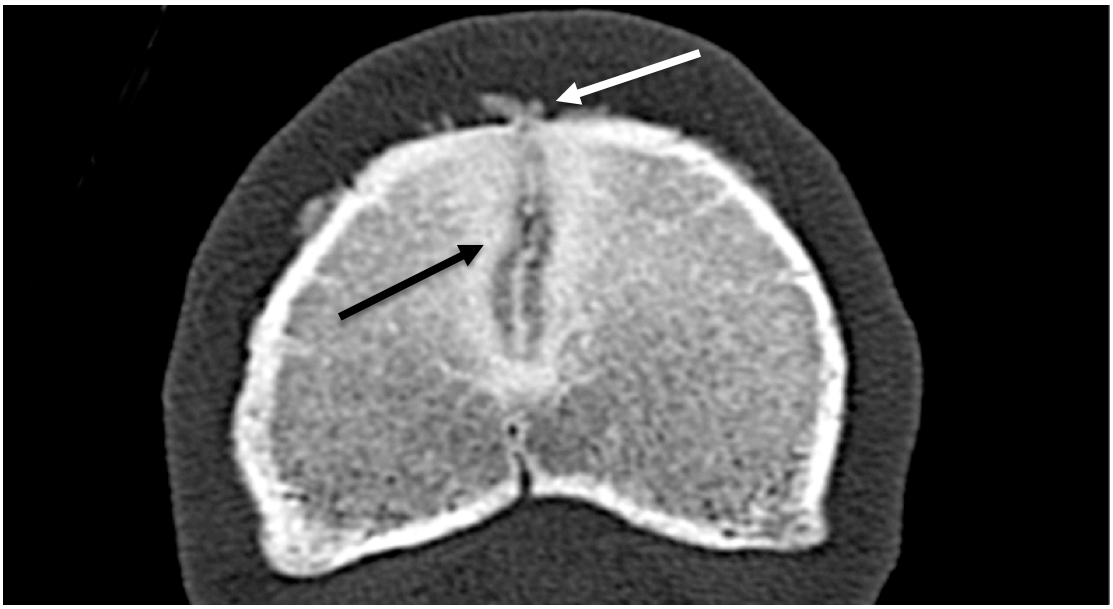

Fig 5c) Transverse CT view of the same SCL showing a clear short incomplete fissure (black arrow) with involvement of the dorsal cortex as well as moderate dorsal periosteal reaction (white arrow). This CT image shows the typical appearance of an SCL in conjunction with a small fissure line with a long split-like opening to the joint surface.

Joints with a cyst and associated fissure had more often periosteal reaction and signs of arthrosis on radiographs (univariate analysis, $p=0.005$ and logistic regression, OR=3.01 and $p=0.024$) and CT scans (univariate analysis, $p=0.011$ and logistic regression, OR=278.70 and $p=0.021$) than joints without a fissure.

Radiography and CT did not differ with respect to the diagnosis of severe PR and OA but subtle PR and OA were detected more frequently on CT scans ($p<0.05$). The CT scans of joints with 2 SCLs showed significantly more often signs of mild OA compared with joints with only one cyst ($p=0.02$), and scans of horses with only one SCL had significantly more often PR (logistic regression, OR=2.80 and $p=0.047$).

3.4 Discussion

The objective of this study was to describe radiographic and computed tomographic characteristics of SCLs that were identified on CT scans and to determine the usefulness of the two techniques for diagnosis of SCLs. Computed tomography allowed excellent assessment of SCLs but only 78% of the cysts detected by CT were seen radiographically, which is in general agreement with the results of other studies.[2,11,13]

Dorsopalmar/plantar radiographic views were best suited for the detection of cystic lesions in the distal limb of horses but larger lesions also were seen on lateromedial or oblique views, which is in agreement with other reports.[5,14] Cysts that were seen on radiographs had significantly more evidence of sclerosis on CT images than cysts that were not visible radiographically. Presumably, sclerosis generated additional contrast that improved radiographic visibility.

Communication between the cyst and joint space was suspected in 74% of cysts seen radiographically and was confirmed in 96% of cysts seen on CT scans. Radiographic identification of these communications is difficult and often only a tentative diagnosis can be made. Radiographic visibility of the communication between cysts in MC III and the joint space was improved using an elevated 45° dorsopalmar view in several horses.[15] A clear gap at the bone-cartilage interface was apparent on CT scans of 43 of 45 cysts, which suggests that a communication between cysts and the joint space is a normal feature of SCLs. However, this was not supported in our previous studies, in which only 30-40% of the SCLs communicated with the joint space.[3,12] In studies of humans with dysplastic osteoarthritic hips, all subchondral cysts detected on CT scans communicated with the joint space.[16,17]

The seemingly common occurrence of cyst-joint space communications favors the synovial fluid intrusion theory of cyst formation. This theory postulates that subchondral bone cysts are the result of degenerative changes in the overlying cartilage, which leads to aberrant communication between the joint space and subchondral bone and forces synovial fluid into

the latter.[17-19] Subchondral cystic lesions close to the joint surface and associated with an articular defect that extends into the subchondral bone are more likely to cause lameness than SCLs located a certain distance from the joint.[12,15] Therefore, the detection of a communicating opening connection between the cyst and joint is clinically significant.

Computed tomography highlights skeletal changes but the quality of the joint cartilage overlying a SCL and the exact nature of the communication between the cyst and the joint cannot be assessed (Fig 6).

Fig 6) Dorsal CT view of an SCL in the distal P2 of the right forelimb in a two-year-old Warmblood mare showing a thin, demarcating, hyperintense line bulging away from the joint surface (white arrow). Scrolling through the CT images a small interruption of this demarcating line was noted, consistent with a communication between the SCL and the distal interphalangeal joint. Additionally a prominent channel connecting the SCL to the medial P2 cortex was detected (black arrow).

Although intra-articular contrast medium can be used to improve the visibility of a communication between the cyst and the joint surface, the results of this technique are often disappointing because the high viscosity of the contrast medium may hamper complete filling of the cyst.[11] Magnetic resonance imaging (MRI) also has limitations for evaluation of joint cartilage in horses; in a study of 40 horses with fetlock lameness, two horses had cartilage lesions in the fetlock that were missed with MRI but detected arthroscopically. The authors of that study felt that cartilage defects are underestimated with MRI.[20] Depending on the joint and the location of the SCL, arthroscopy may show lesions of the joint cartilage that are associated with subchondral bone cysts. Cystic lesions without communication with the joint space are not likely to be detected arthroscopically. Postmortem examination including histology will unambiguously identify the content of the cyst, the condition of the joint cartilage, and the nature of the communication between the cyst and the joint.

Computed tomography scans of 13 SCLs showed a fissure line associated with the cyst but only five of these were seen radiographically. High-quality radiographs taken in several views are crucial for the detection of small fissure lines. Furthermore, if the plane of the fissure does not line up with the x-ray beam or if the changes in the subchondral bone are discrete, a fissure may be missed.[5,21] Acute fissure lines in particular are difficult to diagnose when bone resorption and widening of the fracture line have not yet occurred. In chronic cases, local sclerosis and periosteal new bone formation may suggest a fissure. In this study, fissures were significantly correlated with PR seen on radiographs and CT scans but palmar/plantar periosteal reaction was only seen on CT scans. This illustrates that CT has higher sensitivity than radiography for the assessment of the course and extent of bone fissures and the occurrence of periosteal new bone formation. The simultaneous occurrence of an SCL and a fissure line in almost one third of cases supports the theory that a pre-existing fissure allowed the intrusion of synovial fluid into the subchondral bone through the injured cartilage with subsequent bone resorption because of pressure from the fluid, and subsequent cyst formation.[12,18,22]

Most of the fissure lines had a sagittal course and occurred in the proximal aspect of P1. The mid-sagittal groove seems to predispose the proximal

phalanx to sagittal fracture when undergoing strong torsional force from the sagittal ridge of MC/MT III.[18] This supports the assumption that fissure lines occurred before SCL formation. In a study of ten short incomplete fractures of P1, five fractures were accompanied by an SCL.[18] However, it remains unclear whether a small fissure can lead to the formation of an SCL or whether an SCL causes weakening of the bone with subsequent fissure formation.[9,18,22]

Computed tomographic scans of one third of the SCLs showed characteristic channels between the cysts and the cortex. To our knowledge, such channels have not been documented and we interpreted them as vascular channels, possibly related to increased vascularization associated with bone resorption and remodeling during formation of the cyst.[3]

Computed tomography had higher diagnostic sensitivity for the detection of mild osteoarthritic changes than radiography and changes that were missed radiographically were usually assessed as mild on CT scans. The same was true for mild periosteal changes.

The results of this study showed that CT has several advantages over radiography with respect to the diagnosis of SCLs. Small cysts with no or only a mild sclerotic rim were readily identified using CT but often missed radiographically. Computed tomography revealed a fissure line associated with almost one third of the SCLs and evidence of communication between almost all cysts and the joint space. Channels between the cysts and the cortex, interpreted as vascular channels, were a novel finding and may aid in the clarification of the pathogenesis of SCLs. Lame horses suspected of having an SCL ideally should undergo CT examination to assess the cyst and determine its exact location and the presence of bone fissures and other lesions including periosteal reaction. This facilitates the planning and execution of treatment as well as determining the prognosis.

3.5 References

1. Fuerst A, Kaegi B, von Rechenberg B, et al: Die Behandlung von 5 Pferden mit subchondralen zystoiden Defekten im Fesselbein. Pferdeheilkunde 1997; 13: 147-161.

2. Garcia-Lopez JM, Kirker-Head CA: Occult subchondral osseous cyst-like lesions of the equine tarsocrural joint. Vet Surg 2004; 33: 557-564.

3. von Rechenberg B, McIlwraith CW, Auer JA: Cystic Bone Lesions in Horses and Humans: A Comparative Review. Vet Comp Orthop Traumatol 1998; 11: 8-18.

4. Rijkenhuizen ABM, van den Top GB, van den Belt AJ: The role of computer tomography in the surgical management of cystic lesions. Pferdeheilkunde 2005; 21: 317-321.

5. van Suntum M, Hartung K: Zur Erkennbarkeit subchondraler zystoider Defekte an den distalen Extremitätengelenken des Pferdes. Tierarztl Prax 1989; 17: 79-83.

6. Jacquet S, Audigie F, Denoix JM: Ultrasonographic diagnosis of subchondral bone cysts in the medial femoral condyle in horses. Equine Vet Educ 2007; 19: 47-50.

7. Barrett MF, Zubrod CJ: Use of magnetic resonance imaging to detect and direct therapy of an osseous cystic lesion at the solar surface of the third phalanx of a horse. Equine Vet Educ 2008; 20: 19-23.

8. Zubrod CJ, Schneider RK, Tucker RL, et al: Use of magnetic resonance imaging for identifying subchondral bone damage in horses: 11 cases (1999-2003). J Am Vet Med Assoc 2004; 224: 411-418.

9. Dyson S, Nagy A, Murray R: Clinical and diagnostic imaging findings in horses with subchondral bone trauma of the sagittal groove of the proximal phalanx. Vet Radiol Ultrasound 2011; 52: 596-604.

10. Peterson PR, Bowman KF: Computed Tomographic Anatomy of the Distal Extremity of the Horse. Vet Radiol Ultrasound 1988; 29: 147-156.

11. Barbee DD, Allen JR, Grant BD, et al: Detection by computed tomography of occult osteochondral defects in the fetlock of a horse. Equine Vet J 1987; 19: 556-558.

12. Del Chicca F, Kuemmerle JM, Ossent P, et al: Use of computed tomography to evaluate a fracture associated with a subchondral pedal bone cyst in a horse. Equine Vet Educ 2008; 20: 515-519.

13. Hanson JA, Seeherman HJ, Kirker-Head CA, et al: The role of computed tomography in evaluation of subchondral osseous lesions in seven horses with chronic synovitis. Equine Vet J 1996; 28: 480-488.

14. Deiss E, Fuerst A, Haas C, et al: Symptomatik, Diagnostik und Therpie von 5 Pferden mit traumatischen subchondralen Knochenzysten. Wiener Med Wochenschr 2001; 88: 310-321.

15. Hogan PM, McIlwraith CW, Honnas CM, et al: Surgical treatment of subchondral cystic lesions of the third metacarpal bone: results in 15 horses (1986-1994). Equine Vet J 1997; 29: 477-482.

16. Schmalzried TP, Akizuki KH, Fedenko AN, et al: The role of access of joint fluid to bone in periarticular osteolysis - A report of four cases. J Bone Joint Surg Am 1997; 79A: 447-452.

17. Inui A, Nakano S, Yoshioka S, et al: Subchondral cysts in dysplastic osteoarthritic hips communicate with the joint space: analysis using three-dimensional computed tomography. Eur J Orthop Surg Traumatol 2013; 23: 791-795.

18. Kuemmerle JM, Auer JA, Rademacher N, et al: Short incomplete sagittal fractures of the proximal phalanx in ten horses not used for racing. Vet Surg 2008; 37: 193-200.

19. Auer JA, von Rechenberg B, Fuerst A, et al: Subchondrale Knochenzysten: ein Beitrag zur Ätiologie und Behandlung. Tierarztl Prax 2001; 29: 185 - 193.

20. Gonzalez LM, Schramme MC, Robertson ID, et al: MRI Features of Metacarpo(Tarso) Phalangeal Region Lameness in 40 Horses. Vet Radiol Ultrasound 2010; 51: 404-414.

21. Derungs S, Fuerst A, Haas C, et al: Fissure fractures of the radius and tibia in 23 horses: a retrospective study. Equine Vet Educ 2001; 13: 313-318.

22. Yovich JV, Stashak TS: Subchondral osseous cyst formation after an intra-articular fracture in a filly. Equine Vet J 1989; 21: 72-74.

4 Attachments

Table 1: Statistical values of univariate analysis part 1.

Variable 1	Variable 2	Fisher's
X-ray SCL visibility	X-ray surrounding sclerosis	P = 0.000
X-ray SCL visibility	CT surrounding sclerosis	P = 0.038
X-ray SCL visibility	Distribution of SCLs (2 SCLs within the same joint)	P = 0.002
X-ray OA	CT OA	P = 0.000
X-ray PR	CT PR	P = 0.000
CT OA	Distribution of SCLs (2 SCLs within the same joint)	P = 0.020

Table 2: Statistical values of univariate analysis part 2.

Variable 1	Variable 2	Fisher's
X-ray fissure visibility	X-ray PR	P = 0.005
X-ray fissure visibility	CT PR	P = 0.033
X-ray fissure visbility	CT fissure visbility	P = 0.015
CT fissure visbility	CT OA	P = 0.042
CT fissure visbility	CT PR	P = 0.011
CT fissure visbility	Exact localization fissure (P1)	P = 0.045
CT fissure visbility	Exact localization (sagittal)	P = 0.008

Table 3: Statistical values of multivariate analysis with logistic regression.

Variables	OR	s.e.	P-value	95% CI	
X-ray SCL visibility					
CT surrounding sclerosis	5.66	4.65	0.04	1.13	28.35
Distribution of SCLs (2 SCLs within the same joint)	0.30	0.14	0.01	0.13	0.730
CT connection of SCL to the joint					
Exact localization SCL (P1)	0.80	0.26	0.50	0.42	1.52
X-ray connection of SCL to the joint					
Distribution of SCLs (2 SCLs within the same joint)	0.52	0.17	0.05	0.28	0.99
X-ray fissure visibility					
X-ray PR	3.01	1.47	0.02	1.16	7.82
Exact localization fissure (P1)	4.19	3.23	0.06	0.93	18.97
CT fissure visibility					
X-ray fissure visibility	0.00	0.00	0.01	0.00	0.29
X-ray PR	0.00	0.00	0.02	0.00	0.32
CT PR	278.71	682.34	0.02	2.30	33812.52
CT OA	15.64	21.89	0.05	1.01	243.09
Exact localization SCL (P1)	0.31	0.17	0.03	0.11	0.89
Distribution of SCLs: only 1 SCL					
CT PR	2.81	1.46	0.05	1.01	7.77
Distribution of SCLs: 2 SCL within different limbs					
CT surrounding sclerosis	2.95	1.76	0.07	.92	9.49
Distribution of SCLs: 2 SCL within the same joint					
CT OA	2.07	1.17	0.20	0.68	6.27
Distribution of SCLs: 2 SCL within different joints of the same limb					
CT OA	0.24	0.26	0.19	0.03	2.06

Danksagung

Ich möchte mich an dieser Stelle bei allen Personen ganz herzlich bedanken, welche mich fachlich und persönlich immer unterstützt haben.

Ganz besonders **meinen lieben Eltern**, welche mich in meinem beruflichen Werdegang jederzeit grosszügig unterstützt haben,

Frau **Dr. med. vet. Michelle Jackson**, welche mich mit viel Schwung und Elan in meiner Arbeit unterstützt und ausgebildet hat,

Herrn **Prof. Dr. med. vet. Anton Fürst** für das interessante Thema sowie die Übernahme des Referats,

Herrn **Prof. Dr. med. vet. Patrick R. Kircher** für die Unterstützung seitens der bildgebenden Diagnostik und der Übernahme des Korreferats sowie

Herrn **Prof. Dr. med. vet. Michael Hässig**, für die Hilfe bei der statistischen Auswertung.

Curriculum Vitae

Name:	Stephanie Schön
Geburtsdatum:	13.07.1986
Geburtsort:	Altdorf (UR), Schweiz
Nationalität:	Schweiz
Heimatort:	Menzingen (ZG)

1993 – 2000	Grundschule und Sekundarschule Hochdorf
2000 – 2005	Kantonale Mittelschule Seetal
2005 – 2010	Veterinärstudium an der Vetsuisse-Fakultät Zürich

---

2010 - 2015	Dissertation am Departement für Pferde unter der Leitung von Prof. Dr. med. vet. A. Fürst und der Betreuung von Dr. med. vet. M. Jackson, Vetsuisse-Fakultät Universität Zürich
2010 – 2012	Assistentin an der Vetsuisse-Fakultät Universität Zürich, Klinik für Pferdechirurgie, Departement für Pferde und in der Abteilung für Bildgebende Diagnostik, Departement für Kleintiere
2012 – 2014	Assistentin FVH an der Vetsuisse-Fakultät Universität Zürich, Klinik für Pferdechirurgie, Departement für Pferde
Seit März 2014	Residency ECVS an der Vetsuisse-Fakultät Universität Zürich, Klinik für Pferdechirurgie, Departement für Pferde